

**TRB**

# TRANSPORTATION RESEARCH RECORD

---

Journal of the Transportation Research Board No.1919

Rigid and Flexible  
Pavement Design  
2005

---

TRANSPORTATION RESEARCH BOARD  
*OF THE NATIONAL ACADEMIES*



# TRANSPORTATION RESEARCH RECORD

---

Journal of the Transportation Research Board, No. 1919

**Rigid and Flexible  
Pavement Design  
2005**

A Peer-Reviewed Publication

---

TRANSPORTATION RESEARCH BOARD  
*OF THE NATIONAL ACADEMIES*

Washington, D.C.  
2005

[www.TRB.org](http://www.TRB.org)

**Transportation Research Record 1919**

ISSN 0361-1981  
ISBN 0-309-09392-9

Subscriber Category  
IIB pavement design, management, and performance

Printed in the United States of America

**Sponsorship of Transportation Research Record 1919**

**DESIGN AND CONSTRUCTION GROUP**

Gale C. Page, Florida Department of Transportation (Chair)

**Pavement Management Section**

Nicolaas F. Coetzee, Dynatest Consulting, Inc. (Chair), Judith B. Corley-Lay, Gary E. Elkins, Kenneth W. Fults, Mark P. Gardner, Anastasios M. Ioannides, Thomas J. Kazmierowski, Joe P. Mahoney, Roger C. Olson, James C. Wambold

**Rigid Pavement Design Committee**

Anastasios M. Ioannides, University of Cincinnati (Chair), Jose Tadeu Balbo, Ernest J. Barenberg, Judith B. Corley-Lay, James A. Crovetti, Mostafa Elseifi, Kathleen T. Hall, Michael I. Hammons, Jacob Hiller, Andrew M. Johnson, Lev Khazanovich, Francesca La Torre, David L. Lippert, Andreas Loizos, Robert R. Long, Jr., Aramis Lopez, Jr., James W. Mack, B. Frank McCullough, J. P. Mohsen, Tatsuo Nishizawa, Linda M. Pierce, David W. Pittman, Chetana Rao, Robert Otto Rasmussen, Jeffery R. Roesler, Dulce Rufino, Larry A. Scofield, Kurt D. Smith, Shiraz D. Tayabji, Julie M. Vandenbossche, Gerald F. Voigt, Thomas D. White, Sameh M. Zaghoul

**Flexible Pavement Design Committee**

Kenneth W. Fults, Round Rock, Texas (Chair), Sirous H. Alavi, Gilbert Y. Baladi, Fouad M. Bayomy, Bjorn Birgisson, Albert J. Bush III, Trenton M. Clark, Judith B. Corley-Lay, Bruce Dietrich, Fred N. Finn, Kevin D. Hall, Mustaque Hossain, Andrew M. Johnson, Jiwon Kim, Fenella M. Long, Michael S. Mamlouk, Richard W. May, Walid M. Nassar, David E. Newcomb, Katherine A. Petros, Stephen B. Seeds, Peter J. Stephanos, Marshall R. Thompson, David H. Timm, Per Ullidtz, Harold L. Von Quintus, Kim A. Willoughby, Haiping Zhou

Sponsorship is indicated by a footnote at the end of each paper. The organizational units, officers, and members are as of December 31, 2004.

**Transportation Research Board Staff**

Stephen F. Maher, Engineer of Design  
Michael DeCarmine, Senior Program Associate

**Publications Office**

Chrysa Cullather, Editor; Mark Farrell, Production Editor;  
Mary McLaughlin, Proofreader; Carole O'Connor, Manuscript Preparer  
Ann E. Petty, Managing Editor; Juanita Green, Production Manager;  
Phyllis Barber, Publishing Administrator; Jennifer J. Weeks, Manuscript Preparation Manager

# Transportation Research Record 1919

---

## Contents

Foreword	vii
<hr/>	
<b>PART 1—RIGID PAVEMENTS</b>	
<b>Closed-Form, Six-Slab, Thick-Plate Solution for Analysis of Edge Slab of Concrete Pavement</b> Liu Wei and T. F. Fwa	<b>3</b>
<hr/>	
<b>Engineering Solution for the Uniform Strength of Partially Cracked Concrete</b> Elin A. Jensen, Will Hansen, and Rune Brincker	<b>16</b>
<hr/>	
<b>Improvements of Testing Procedures for Concrete Coefficient of Thermal Expansion</b> Moon Won	<b>23</b>
<hr/>	
<b>Enhanced Portland Cement Concrete Fatigue Model for StreetPave</b> Leslie Titus-Glover, Jagannath Mallela, Michael I. Darter, Gerald Voigt, and Steve Waalkes	<b>29</b>
<hr/>	
<b>Measurement and Significance of the Coefficient of Thermal Expansion of Concrete in Rigid Pavement Design</b> Jagannath Mallela, Ala Abbas, Tom Harman, Chetana Rao, Rongfang Liu, and Michael I. Darter	<b>38</b>
<hr/>	
<b>Stress Prediction for Cracking of Jointed Plain Concrete Pavements, 1925–2000: An Overview</b> Anastasios M. Ioannides	<b>47</b>
<hr/>	
<b>Concrete-Filled, Glass Fiber-Reinforced Polymer Dowels for Load Transfer in Jointed Rigid Pavements</b> Scott Murison, Ahmed Shalaby, and Aftab Mufti	<b>54</b>
<hr/>	

<b>Estimating the Sensitivity of Design Input Variables for Rigid Pavement Analysis with a Mechanistic–Empirical Design Guide</b>	<b>65</b>
Kevin D. Hall and Steven Beam	

---

## **PART 2—FLEXIBLE PAVEMENTS**

<b>Calibration of Alligator Fatigue Cracking Model for 2002 Design Guide</b>	<b>77</b>
Mohamed M. El-Basyouny and Matthew Witczak	

---

<b>Field and Theoretical Evaluation of Thermal Fatigue Cracking in Flexible Pavements</b>	<b>87</b>
Imad L. Al-Qadi, Marwa M. Hassan, and Mostafa A. Elseifi	

---

<b>Predicting Asphalt Pavement Temperature with a Three-Dimensional Finite Element Method</b>	<b>96</b>
Manuel J. C. Minhoto, Jorge C. Pais, Paulo A. A. Pereira, and Luis G. Picado-Santos	

---

<b>Analytical Study of Effects of Truck Tire Pressure on Pavements with Measured Tire–Pavement Contact Stress Data</b>	<b>111</b>
Randy B. Machemehl, Feng Wang, and Jorge A. Prozzi	

---

<b>Implementing the Mechanistic–Empirical Design Guide Procedure for a Hot-Mix Asphalt–Rehabilitated Pavement in Indiana</b>	<b>121</b>
Khaled A. Galal and Ghassan R. Chehab	

---

<b>Quantification of the Joint Effect of Wheel Load and Tire Inflation Pressure on Pavement Response</b>	<b>134</b>
Jorge A. Prozzi and Rong Luo	

---

<b>Implementation Initiatives of the Mechanistic–Empirical Pavement Design Guides in Indiana</b>	<b>142</b>
Tommy Nantung, Ghassan Chehab, Scott Newbolds, Khaled Galal, Shuo Li, and Dae Hyeon Kim	

---

<b>Strategic Plan of the Texas Department of Transportation for Implementing NCHRP 1-37A Pavement Design Guide</b>	<b>152</b>
Jacob Uzan, Thomas J. Freeman, and Gregory S. Cleveland	

---

<b>Evaluation of Predicted Pavement Response with Measured Tire Contact Stresses</b>	<b>160</b>
Dae-Wook Park, Emmanuel Fernando, and Joe Leidy	

---

# Foreword

The 2005 series of the *Transportation Research Record: Journal of the Transportation Research Board* consists of approximately 770 papers selected from 2,600 submissions after rigorous peer review. The peer review for each paper published in this volume was coordinated by the sponsoring committee acknowledged at the end of the text; members of the sponsoring committees for the papers in this volume are listed on page ii. Many of these papers were presented at the TRB 84th Annual Meeting in January 2005, and draft versions were included in the Annual Meeting Compendium of Papers CD-ROM.

Additional information about the *Transportation Research Record: Journal of the Transportation Research Board* series and the peer review process appears on the inside back cover. TRB appreciates the interest shown by authors in offering their papers, and the Board looks forward to future submissions.

# Predicting Asphalt Pavement Temperature with a Three-Dimensional Finite Element Method

Manuel J. C. Minhoto, Jorge C. Pais,  
Paulo A. A. Pereira, and Luis G. Picado-Santos

A three-dimensional (3D) finite element (FE) model was developed to calculate the temperature of a pavement located in northeast Portugal. A case study was developed to validate the model. Input data to the model were the hourly values for solar radiation and temperature and mean daily values of wind speed obtained from a meteorological station. The thermal response of a multilayered pavement structure was modeled with a transient thermal analysis for 4 months (December 2003 to April 2004), and the analysis was initiated with the full-depth constant initial temperature obtained from field measurements. During these 4 months, the pavement temperature was measured at a new pavement section, located in IP4 main road, near Bragança, in northern Portugal. At this location, seven thermocouples were installed in the asphalt concrete layers at seven different depths. These pavement data were used to validate this simulation model by a comparison of model calculated data with measured pavement temperatures. The 3D FE analysis proved to be an interesting tool to simulate the transient behavior of asphalt concrete pavements. The suggested simulation model can predict the pavement temperature at different levels of bituminous layers with good accuracy.

Bituminous overlays have been the most common method of pavement rehabilitation. In an overlay placed on a cracked pavement, the cracks will develop and propagate to the pavement surface directly above cracks in the existing pavement under static and repetitive loading during the first few years of service. This mode of distress is traditionally referred to as "reflective cracking" and is a major concern to highway agencies throughout the world. Thus, the asphalt concrete overlay is exposed to great strains and stresses when subjected to traffic and thermal loadings. Several authors (1, 2) suggest different mechanisms as the origin and propagation of cracks in overlays of pavements:

1. Thermal stresses from thermal fatigue occur when temperature variations induce cyclic openings and closures of cracks in the pavement, which induce stress concentrations in the overlay.
2. Thermal stresses result from rapid cooling of the top layer, which induces critical tensile stresses on overlay.

M. J. C. Minhoto, Superior School of Management and Technology, Bragança Polytechnic Institute, Campus de Santa Apolónia, Apartado 134, 5301-857 Bragança, Portugal. J. C. Pais and P. A. A. Pereira, Department of Civil Engineering, University of Minho, Campus Azurém, 4800-058 Guimarães, Portugal. L. G. Picado-Santos, Department of Civil Engineering, Foundation for Science and Technology, University of Coimbra, Polo 2, 3030 Coimbra, Portugal.

*Transportation Research Record: Journal of the Transportation Research Board*, No. 1919, Transportation Research Board of the National Academies, Washington, D.C., 2005, pp. 96-110.

3. Repetitive traffic loads induce additional distress in the overlay and increase the rate of crack propagation, whether or not these cracks originate from thermal stresses.

4. Compressive stresses or strains occur at the top of the unbound materials, when the failure mechanism is likely to be something other than reflective or fatigue cracking.

The literature review (2) also revealed that daily and seasonal temperature variations, as well as the associated thermal stresses, could be a cause of premature overlay cracking, which affects the predictive overlay service life of asphalt concrete (AC) layers. In regions that experience large daily temperature variations or extremely low temperatures, the thermal conditions play a major role in reflective cracking response of a multilayered pavement structure. On the one hand, binder properties (e.g., stiffness, ageing, penetration) are sensitive to temperature variations. On the other hand, the combination of the two most important effects—wheel loads passing above (or near) the crack and the tension increase in the material above the crack (in the overlay) because of rapidly decreasing of temperatures—have been identified as the most likely causes of high states of stress and strain above the crack and is most likely responsible for the reflective cracking (3).

Daily temperature variations have an important influence on the pavement thermal state at a depth of a few decimeters below the surface. Depending on the temperature variation level, stresses are induced in the overlay in two different ways, which need to be distinguished: through restrained shrinkage of the overlay and through the existing movements of slabs caused by the thermal shrinking phenomenon.

To calculate the pavement thermal effects and the thermal response of the AC mixes, it is necessary to evaluate the temperature distribution evolution on many depths of bituminous layers throughout typical 24-h periods. The temperature distributions obtained for different hours during the day allow for the calculation of thermal effects in the zone above the crack; they can be used to investigate other effects, such as the temperature influence on properties of layer materials (like stiffness).

The time variation of pavement thermal state is controlled by climatic conditions, thermal diffusivity of the materials, thermal conductivity, specific heat, density, and the depth below the surface (2, 4). The temperature distribution on a pavement structure can be obtained through field measurements using temperature-recording equipment (Datalogger associated with thermocouples) or can be estimated by using mathematical models. The option of using the field measurement is desirable because actual temperature can be reliably measured and used in stress calculation models. However, this method is relatively

slow and provides information about temperatures in the observed period only. Conversely, a temperature theoretical model may suffer slightly because of a lack of accuracies but will give a temperature distribution quickly and cheaply and can be used to predict temperature distributions under a wide range of conditions, including any unusual or extreme conditions.

The simulation model suggested in this paper is based on the finite element (FE) method, which involves weather data as input. The simulation model was validated by comparing the calculated temperatures with measured pavement temperatures obtained from December 2003 to April 2004. The model computes the pavement temperatures by using measured climate data values as input for the same time period.

Although this thermal approach may have the nature of a one-dimensional problem of the heat conduction in the vertical direction, given the infinite nature in the horizontal direction, the suggested model was developed on a 3D basis, having in view its future compatibility with a 3D mechanical reflective cracking model used by the authors in other projects.

**BACKGROUND**

To develop the pavement temperatures prediction model, basic principles needed to be adopted. The following sections present the main principles adopted in the proposed model once the hourly temperature distribution was governed by heat conduction principles within pavement and by energy interaction between the pavement and its surroundings.

**Conduction Heat Transfer**

Conjugating the first law of thermodynamics, which states that thermal energy is conserved, and Fourier’s law, which relates the heat flux with the thermal gradient, the problem of heat transfer by conduction within the pavement is solved. For an isotropic medium and for constant thermal conductivity, this adopted principle is expressed as follows (5, 6):

$$\nabla^2 T = \frac{1}{\alpha} \times \left( \frac{\partial T}{\partial t} \right) \tag{1}$$

where

$$\nabla^2 = (\partial^2/\partial x^2) + (\partial^2/\partial y^2) + (\partial^2/\partial z^2),$$

$$\alpha = \frac{k}{\rho \times C} = \text{thermal diffusivity,}$$

*k* = thermal conductivity,

$\rho$  = density,

*C* = specific heat,

*T* = temperature,

*t* = time, and

*x*, *y*, and *z* = components of the Cartesian coordinate system.

**Interaction Between Pavement and Surroundings**

On a sunny day, the heat transfer by energy interaction between the pavement and its surroundings consists of radiation balance

and exchanges by convection. The radiation balance (or thermal radiation) involves the consideration of outgoing longwave radiation, longwave counterradiation, and shortwave radiation (or solar radiation) (7).

The earth surface is assumed to emit longwave radiation as a black body. Thus, the outgoing longwave radiation follows the Stefan–Boltzman law (5, 7):

$$q_e = \epsilon_e \sigma T_{sur}^4 \tag{2}$$

where

*q<sub>e</sub>* = outgoing radiation,

$\epsilon_e$  = emission coefficient,

$\sigma$  = Stefan–Boltzman constant, and

*T<sub>sur</sub>* = pavement surface temperature.

As the atmosphere absorbs radiation and emits it as longwave radiation to the earth, this counterradiation absorbed by the pavement surface is calculated as proposed by Hermansson (7) and Dewitt and Incropera (5):

$$q_a = \epsilon_a \sigma T_{air}^4 \tag{3}$$

where

*q<sub>a</sub>* = absorbed counterradiation,

$\epsilon_a$  = pavement surface absorptivity for longwave radiation and the amount of clouds, and

*T<sub>air</sub>* = air temperature.

Several authors (4, 8) consider the longwave radiation intensity balance (or thermal radiation) through the following expression:

$$q_r = h_r (T_{sur} - T_{air}) \tag{4}$$

where *q<sub>r</sub>* is longwave radiation intensity balance, and *h<sub>r</sub>* is the thermal radiation coefficient. The expression used to obtain *h<sub>r</sub>* is as follows (4):

$$h_r = \epsilon \sigma (T_{sur} + T_{air}) (T_{sur}^2 + T_{air}^2) \tag{5}$$

where  $\epsilon$  is the emissivity of the pavement surface.

Part of the high-frequency (shortwave) radiation emitted by the sun is diffusely scattered in the atmosphere of the earth in all directions, and the diffuse radiation that reaches the earth is called diffused incident radiation. The radiation from the sun reaching the earth surface, without being reflected by clouds or absorbed or scattered by atmosphere, is called direct incident shortwave radiation. The total incident radiation (direct and diffused) can be estimated using the following equation (4–6):

$$q_i = \eta s_c f \cos \theta \tag{6}$$

where

*q<sub>i</sub>* = thermal incident solar radiation,

$\eta$  = loss factor accounting for scattering and absorption of shortwave radiation by atmosphere,

*s<sub>c</sub>* = solar constant, assumed to be 1,353 W/m<sup>2</sup>,

*f* = factor accounting for the eccentricity of earth orbit, and

$\theta$  = zenith angle.

The effective incident solar radiation absorbed by pavement surface may be determined by the following equation (8):

$$q_s = \alpha_s \times q_i \quad (7)$$

where  $q_i$  is the incident solar radiation absorbed by the pavement surface and  $\alpha_s$  is the solar radiation absorption coefficient.

In the model suggested in this paper, shortwave radiation is given as input data obtained measured values. The convection heat transfer between the pavement surface, and the air immediately above is given as follows (4, 7):

$$q_c = h_c(T_{sur} - T_{air}) \quad (8)$$

where  $q_c$  is convection heat transfer and  $h_c$  is the convection heat transfer coefficient. The convection heat transfer coefficient can be calculated as follows:

$$h_c = 698.24 \left\{ [1.44 \times 10^{-4} T_{ave}^{0.5} U^{0.7}] + [9.7 \times 10^{-4} (T_{sur} - T_{air})^{0.3}] \right\}$$

where  $T_{ave}$  is the average temperature given by  $T_{ave} = (T_{sur} - T_{air})/2$  and  $U$  is the wind speed.

### FINITE DIFFERENCE METHODOLOGY

The transient temperature response of pavements may be analyzed through a numerical incremental recursive model, using the finite differences method, by applying the energy balance principle and the Fourier heat transfer equation. The thermal conductivity and thermal diffusivity of pavement are estimated through a convergence process.

The discrete form of Fourier equations within the layer can be written as follows (4):

$$K_i \left( \frac{T_{m-1}^p - T_m^p}{\Delta z} \right) - K_i \left( \frac{T_m^p - T_{m+1}^p}{\Delta z} \right) = \rho C \left( \frac{T_m^{p+1} - T_m^p}{\Delta t} \right) \Delta z \quad (9)$$

where

- $\Delta t$  = time increment;
- $\Delta z$  = depth increment;
- $p$  = time superscript, such that  $|T^{p+1} - T^p| = \Delta t$ ;
- $m$  = depth subscript, such that  $|z_{m+1} - z_m| = \Delta z$ ;
- $K_i$  = thermal conductivity coefficient of layer  $i$ ; and
- $T_m^p$  = temperature in the node  $m$  at time  $p$ .

The discrete form of Fourier equations in the interface zone of layers can be written as follows (4):

$$T_m^{p+1} = \frac{2\Delta t}{r(\Delta z)^2} (K_i + T_{m+1}^p + K_{i+1}T_{m+1}^p) + \left[ 1 - \frac{2K_i \Delta t}{r(\Delta z)^2} - \frac{2K_{i+1} \Delta t}{r(\Delta z)^2} \right] T_m^p \quad (10)$$

where  $r = C_i \rho_i + C_{i+1} \rho_{i+1}$ . Interaction between the pavement and its surroundings at surface ( $z = 0$ ) can be written as follows (4):

$$h_c(T_{sur} - T_{air}^p) + q_s + h_c(T_{sur} - T_{air}^p) + K_i \left( \frac{T_1^p - T_{sur}^p}{\Delta z} \right) = \rho C \frac{\Delta z}{2} \left( \frac{T_{sur}^{p+1} - T_{sur}^p}{\Delta t} \right) \quad (11)$$

An Excel spreadsheet was developed to solve the transient state temperature model using the finite differences method. The equations were

solved incrementally at each 30-s time step to predict temperature at any given depth at a given time step. The model solution requires the determination of initial temperature distribution in the layer system before transient analysis. The initial temperature distribution adopted was obtained from field measurements.

### FE METHOD

This study is based on the use of the FE method in the prediction of temperature distributions in AC pavements. In the last several years, this methodology has been revealed to be a tool of great applicability in the pavement research domain.

### Conduction

The first law of thermodynamics, which states that thermal energy is conserved, was used to build the solution of the pavement thermal problem through FEs. Considering a differential control volume of a pavement, in that methodology, the conservation of thermal energy is expressed by Equation 12:

$$\rho C \frac{\partial T}{\partial t} + \{L\}^T \{q\} = 0 \quad (12)$$

where

$T$  = temperature =  $T(x, y, z, t)$ ,

$$\{L\} = \begin{Bmatrix} \frac{\partial}{\partial x} \\ \frac{\partial}{\partial y} \\ \frac{\partial}{\partial z} \end{Bmatrix} = \text{vector operator, and}$$

$\{q\}$  = heat flux vector.

The term  $\{L\}^T \{q\}$  also may be interpreted as  $\nabla \cdot \{q\}$ , where  $\nabla$  represents the divergence operator. Fourier's law can be used to relate the heat flux vector to the thermal gradients through the following expression:

$$\{q\} = -[D]\{L\}T \quad (13)$$

where

$$[D] = \begin{bmatrix} K_{xx} & 0 & 0 \\ 0 & K_{yy} & 0 \\ 0 & 0 & K_{zz} \end{bmatrix}$$

is the conductivity matrix and  $K_{xx}$ ,  $K_{yy}$ ,  $K_{zz}$  are the thermal conductivity in the element  $x$ ,  $y$ , and  $z$  directions, respectively.

Expanding equation to its more familiar form gives the following:

$$\rho C \frac{\partial T}{\partial t} = \frac{\partial}{\partial x} \left( K_{xx} \frac{\partial T}{\partial x} \right) + \frac{\partial}{\partial y} \left( K_{yy} \frac{\partial T}{\partial y} \right) + \frac{\partial}{\partial z} \left( K_{zz} \frac{\partial T}{\partial z} \right) \quad (14)$$

Considering the isotropy of material ( $K = K_{xx} = K_{yy} = K_{zz}$ ) yields the following:

$$\rho C \frac{\partial T}{\partial t} = \frac{\partial}{\partial x} K \left[ \left( \frac{\partial T}{\partial x} \right) + \frac{\partial}{\partial y} \left( \frac{\partial T}{\partial y} \right) + \frac{\partial}{\partial z} \left( \frac{\partial T}{\partial z} \right) \right] \quad (15)$$

**Boundary Conditions**

Three types of boundary conditions, which cover the entire model, were considered: heat flow acting over the model surface limits, surface convection applied in the superior surface of model, and the radiant energy between the model superior surface and its surroundings.

Specified heat flow acting over a surface follows the general expression shown in Equation 16:

$$\{q\}^T \{\eta\} = -q^* \tag{16}$$

where  $\{\eta\}$  is the unit outward normal vector and  $q^*$  is the specified heat flow.

Specified convection-surfaces heat flows acting over a surface follows the general expression shown in Equation 17:

$$\{q\}^T \{\eta\} = h_f(T_{sur} - T_{air}) \tag{17}$$

where

- $h_f$  = convection coefficient,
- $T_{sur}$  = temperature at the surface of the model, and
- $T_{air}$  = bulk temperature of the adjacent fluid.

Radiant energy exchange between a surface of the model and its surroundings is translated by the following expression, which gives the heat transfer rate between the surface and a point representing the surroundings:

$$q_r = \sigma \epsilon (T_{sur}^4 - T_{air}^4) \tag{18}$$

**3D FE METHOD PAVEMENT THERMAL MODEL**

The 3D FE method (FEM) was used to model the thermal behavior of pavement. The pavement structures traditionally are idealized as a set of horizontal layers of constant thickness; homogeneous, continuous, and infinite in the horizontal direction; resting on a subgrade; and semi-infinite in the vertical direction. The thermal configuration of the pavement model was defined based on those principles and is presented in Figure 1. This model considers the possibility of data production for a mechanical model with the same mesh.

The adopted mesh also has been designed for study of the reflective cracking phenomenon caused by the traffic loading and represents an existing pavement, in which a crack is simulated through an element with zero-stiffness and a layer on top of the existing pavement represents an overlay. This mesh was described in other works by the authors (9).

The FEM used in numerical thermal analysis was performed using a general FEs analysis source code, ANSYS 5.6 (10). This analysis is a 3D transient analysis, using a standard FE discretization of the pavement. In the design of the thermal FE mesh, the compatibility of mesh with other mechanical models was observed.

The following factors have been considered in the design of the FE mesh:

- A finer element size is adopted closer to the pavement surface and closer to the wheel load zone, where stress gradient may be highest.

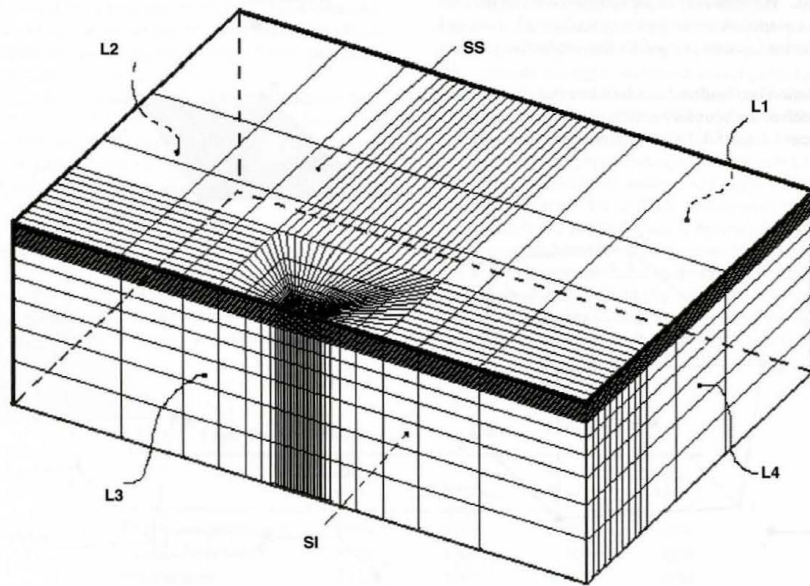


FIGURE 1 FEM mesh thermal model (L1–L4 and SI are boundary surfaces of model and SS represents pavement surface).

- A finer element size is required in the overlay above the crack.
- Because of the symmetry, only half of the model needs to be modeled, which reduces the time consumed in the computing process.

After designed mesh, the number of elements was 13,538. For 3D thermal analysis, a 3D solid element, SOLID70, was used (Figure 2). This element (applicable to a 3D transient thermal analysis) has the capability for 3D thermal conduction, according to the previous explanation. The element has eight nodes with a single degree of freedom (temperature) at each node.

The thermal properties of pavement material (e.g., thermal conductivity, specific heat, and density) for each pavement layer were defined in the "material properties" of this element, when the model was developed. For surface effect applications, such as radiation exchanges by convection heat transfer, the surface element SURF152 was used. The geometry, node locations, and the system coordinates for this element are shown in Figure 3.

The element is defined by four nodes and by material properties. An extra node (away from the base element) is used to simulate the effects of convection and radiation and represents the point where the hourly air temperature is introduced (representing the atmosphere). It was overlaid onto an area face of 3D thermal element SOLID70, as shown in Figure 4. The element is applicable to 3D thermal analysis and allows these load types and surface effects, such as heat fluxes, to exist simultaneously. The surface elements were placed on the entire surface SS (Figure 1).

The convection coefficient (or film coefficient) must be used to consider surface convection in the conductivity matrix calculation. When an extra node is used, its temperature becomes the air temperature. This element allows for radiation between the surface and the extra node "M." The emissivity of the surface is used for the conductivity matrix calculation, for considering surface radiation, and the Stefan-Boltzman constant is used for the conductivity matrix calculation.

The solar radiation is considered as a heat flux that is applied on surface SS. To define the boundary conditions, a null heat flux is applied on surfaces L1, L2, L3, L4, and SI, presented in Figure 1.

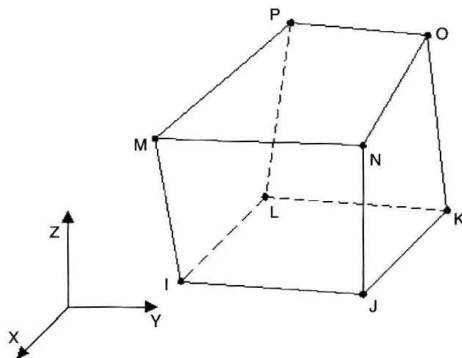


FIGURE 2 3D thermal solid element (SOLID70) (I-P are element nodes).

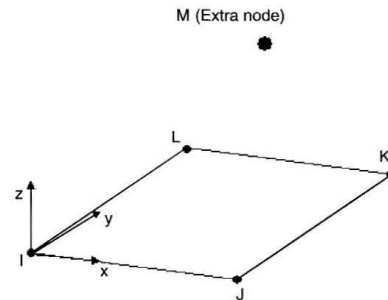


FIGURE 3 Surface thermal element (SURF152) (I-M are element nodes).

**PAVEMENT TEMPERATURE PREDICTION—CASE STUDY**

The main goal of this study was to validate an FEM simulation model developed to calculate the temperatures of a pavement. A FEM numerical analysis for the distribution of temperature in a full-depth asphalt pavement in a trial section located on km 197.700 of IP4 (Bragança, Portugal) was performed for the weather conditions (air temperature, solar radiation, and wind speed) from December 2003 to June 2004.

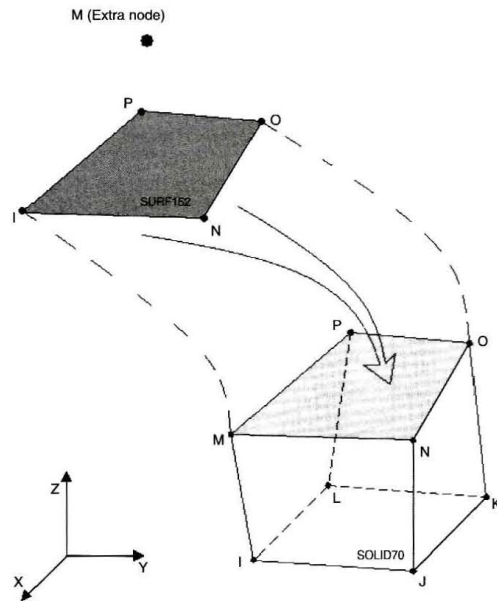


FIGURE 4 SURF152 and SOLID70 coupling (I-P are element nodes).

The model validation was made by statistical analysis between the FEM numerical temperature results, finite differences temperature results, and the field-measured temperatures.

### Field Data Collection

For 4 months (December 2003 to April 2004), pavement temperatures were measured at a new pavement section, located at IP4 main road, near from Bragança, in the north of Portugal. At that location, seven thermocouples were installed in the AC layer at seven different depths: 0, 27.5, 55, 125, 165, 220, and 340 mm. The top thermocouple was installed just at the pavement surface. The depths for the other six were chosen to give a good representation of the whole AC layers at different locations. AC temperatures were recorded every hour of every day.

With respect to short-term temperature response, it can be argued that subgrade temperature at 2.0-m depth is reasonably constant over a given month. The hourly measurements of weather parameters, such as air temperature, solar radiation intensity, and wind speed, were obtained from a meteorological station located near the test pavement section. These measurements were used as input data in the simulation models to carry out temperature distribution prediction in a 340-mm full-depth pavement.

### Input Data to Simulation

The pavement surface thermal emissivity for estimating the long-wave radiation intensity balance was equal to 0.9, and the solar absorption coefficient was equal to 0.95. Table 1 presents the values for the pavement material thermal properties adopted in this study. The parameters have been adapted to give a good correspondence between calculated and measured pavement temperatures. The adopted values follow the typical values for those parameters suggested by previous research (2–4, 7).

As expressed in the conclusions obtained from a simulation made by Hermansson (7), the influence of the thermal conductivity of the pavement is marginal for the pavement temperatures close to the surface. Thus, no further effort was made in this paper to study the influence of thermal conductivity variation.

### Analysis Procedure

The thermal response of the FEM simulation model, representing a multilayered pavement structure, was modeled using a transient thermal analysis for 4 months (from December 2003 to April 2004). This

is the best period (winter) of analysis to study the reflective cracking phenomenon, subjected to influence of temperature variations. It was assumed that the pavement hourly temperature profile depended entirely on hourly air temperature value, hourly solar radiation value, and wind speed daily mean value.

The analysis procedure involved multiple 3D FE runs and was initiated with the full depth at constant initial temperature, obtained from field measurements. The analysis procedure was carried out for a period between December 2003 and April 2004, with a periodicity of 1 h. The thermal response analysis performed by the finite differences method was made for the same conditions used in the finite element method.

### RESULTS

As a measure of error, the absolute difference between calculated and measured pavement temperatures was calculated for every hour. Then the average difference was determined for each month and for the total time period, which is assigned as average error. Table 2 presents the result of this procedure, and Table 3 presents the standard deviation of errors. Figures 5 to 11 present the temperature distributions in the months of January and April 2004, located at surface, 55-mm depth, and 165-mm depth, and March for 55-mm depth where a good correlation was obtained between the in situ measurements and the calculated temperature.

### CONCLUSIONS

The 3D FE analysis has proved to be an interesting tool to simulate the transient behavior of asphalt concrete pavement temperature. According to comparisons performed with field measurements, the suggested simulation model can model the pavement temperature at different levels of bituminous layers with good accuracy. To obtain this distribution, a series of climatic data is needed as an input to the model. The use of the results for other FEM mechanical models constitutes a great advantage of the proposed model.

In comparison of measured and calculated temperature data for every hour for 4 months, an average error less than 2.1°C was obtained in the depths close to the surface. At a depth of 340 mm, the average error may reach 4°C in April. In cold months, the average error is less than in hot months. Thus, in the cold months, the developed model presents better performance than in hot months.

The average error produced by the FEM simulation model is closer to the average error produced by finite difference methodology. The small error variations observed between these models can be caused by the consideration of the average wind speed in FEM model. The

TABLE 1 Layer Thermal Properties

	Thickness (m)	K (W/°C.m)	C (W.s/kg.°C)	Density (kg/m <sup>3</sup> )
Overlay—wearing course	0.055	1.5	850	2550
Overlay—base course	0.070	1.5	860	2350
Cracked layer	0.215	1.5	850	2550
Subbase	0.300	1.5	805	2370
Subgrade	—	1.79	1100	2200

**TABLE 2 Average Error Results**

		Average Errors (degree C)													
Depth >		0 mm		27.5 mm		55 mm		125 mm		165 mm		220 mm		340 mm	
Month	Method >	Fin. Diff.	FEM	Fin. Diff.	FEM	Fin. Diff.	FEM	Fin. Diff.	FEM	Fin. Diff.	FEM	Fin. Diff.	FEM	Fin. Diff.	FEM
December		1.7305	2.1892	1.5251	1.9867	1.3084	1.7164	1.1059	1.3043	1.184	1.0978	1.4373	0.9521	2.6714	2.1224
January		1.6697	1.6985	1.4632	1.5323	1.3639	1.3754	1.2304	1.1993	0.9665	0.9327	0.7856	0.7229	1.7828	1.9414
February		1.3608	1.3675	1.1767	1.2076	1.062	1.0318	0.7143	0.7055	1.0661	0.9145	0.7122	0.6951	2.613	2.4323
March		1.3604	1.3878	1.1726	1.2091	1.2069	1.179	1.5942	1.3959	1.8198	1.4972	1.0481	0.8016	2.8134	2.647
April		2.0394	2.0085	1.9417	2.0141	1.7611	1.6663	2.0518	1.8459	2.2845	1.9264	1.4738	1.2073	4.2292	4.0886
December–April		1.6441	1.6825	1.4745	1.5572	1.3719	1.3665	1.4168	1.3238	1.5311	1.3234	1.0538	0.8773	2.8677	2.7632

NOTE: Fin. Diff. = finite differences.

**TABLE 3 Standard Deviation of Error Results**

		Standard Deviation of Errors (degree C)													
Depth >		0 mm		27.5 mm		55 mm		125 mm		165 mm		220 mm		340 mm	
Month	Method >	Fin. Diff.	FEM	Fin. Diff.	FEM	Fin. Diff.	FEM	Fin. Diff.	FEM	Fin. Diff.	FEM	Fin. Diff.	FEM	Fin. Diff.	FEM
December		1.1553	1.5899	0.9263	1.3457	0.9026	1.0678	0.9149	0.7346	0.9236	0.6562	0.6885	0.64	1.6151	1.0578
January		1.3382	1.3795	1.202	1.2571	1.0186	1.0798	0.8126	0.8333	0.6854	0.7742	0.5209	0.6305	1.3446	1.1094
February		1.0773	1.0843	0.82	0.8782	0.7761	0.7716	0.5463	0.5452	0.7522	0.6973	0.5073	0.4846	1.7641	1.4332
March		1.2977	1.3246	0.9796	1.0594	1.0747	1.0601	1.1578	1.1019	1.3582	1.1674	0.9383	0.8001	2.1728	2.0396
April		1.6421	1.6259	1.312	1.3569	1.2859	1.2365	1.3	1.2326	1.7471	1.4497	0.8732	0.7271	2.8718	2.6089
December–April		1.3871	1.4314	1.1469	1.2349	1.0899	1.0955	1.1144	1.0416	1.3367	1.1404	0.8002	0.7045	2.2874	2.0395

NOTE: Fin. Diff. = finite differences.

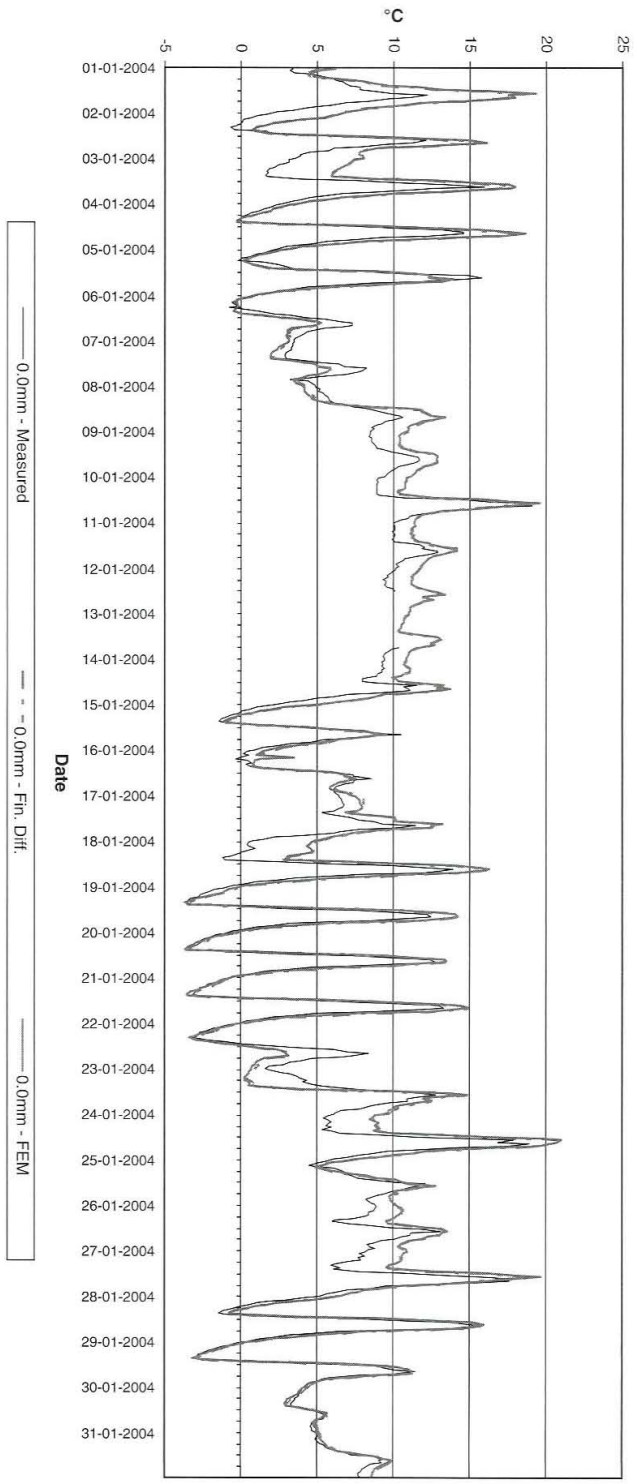


FIGURE 5 January 0.0mm depth temperature distribution (Fin. Diff. = finite differences method).

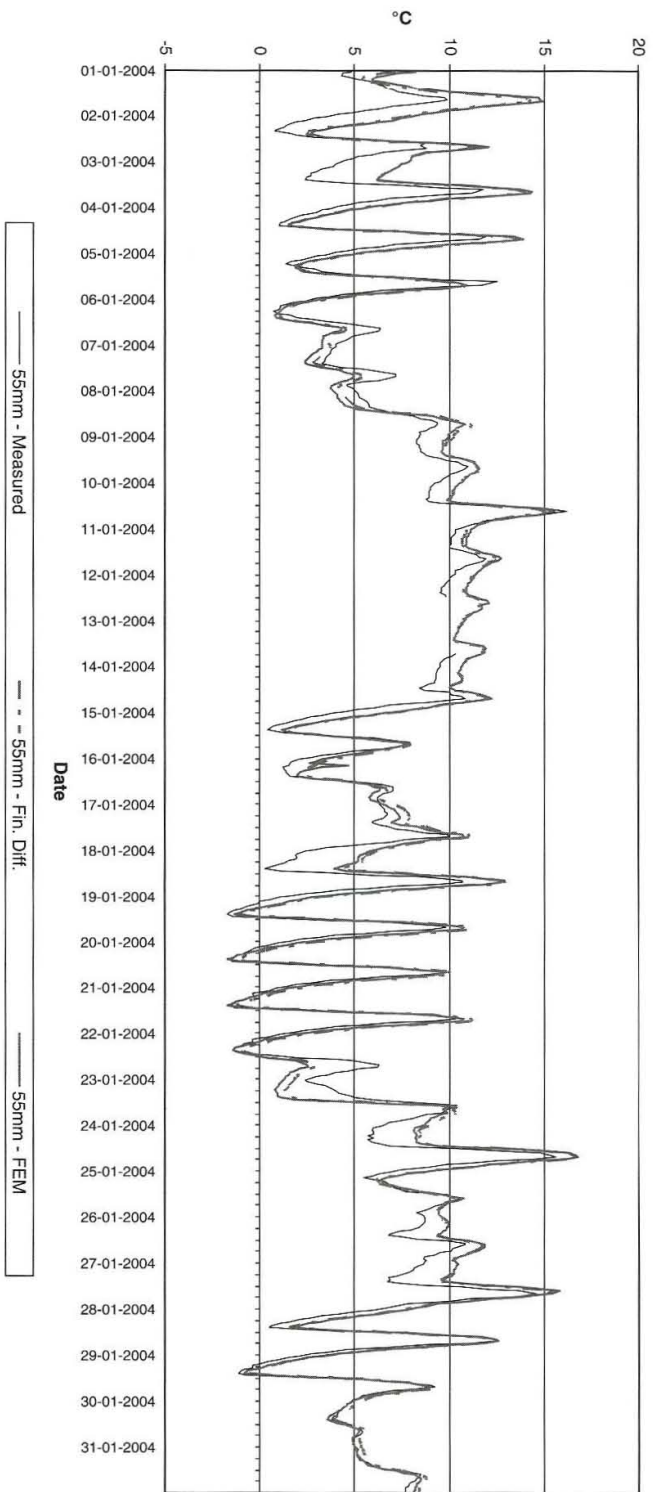


FIGURE 6 January 55-mm depth temperature distribution (Fin. Diff. = finite differences method).

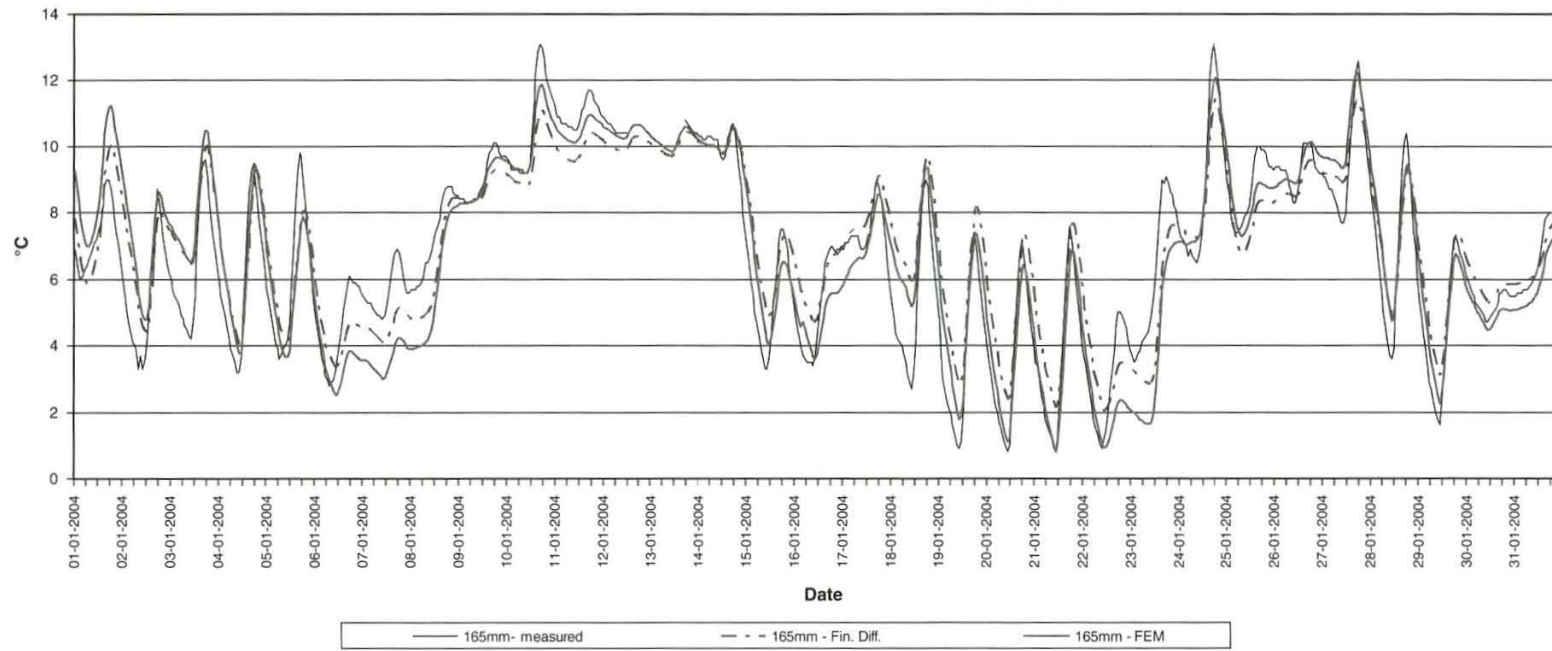


FIGURE 7 January 165-mm depth temperature distribution (Fin. Diff. = finite differences method).

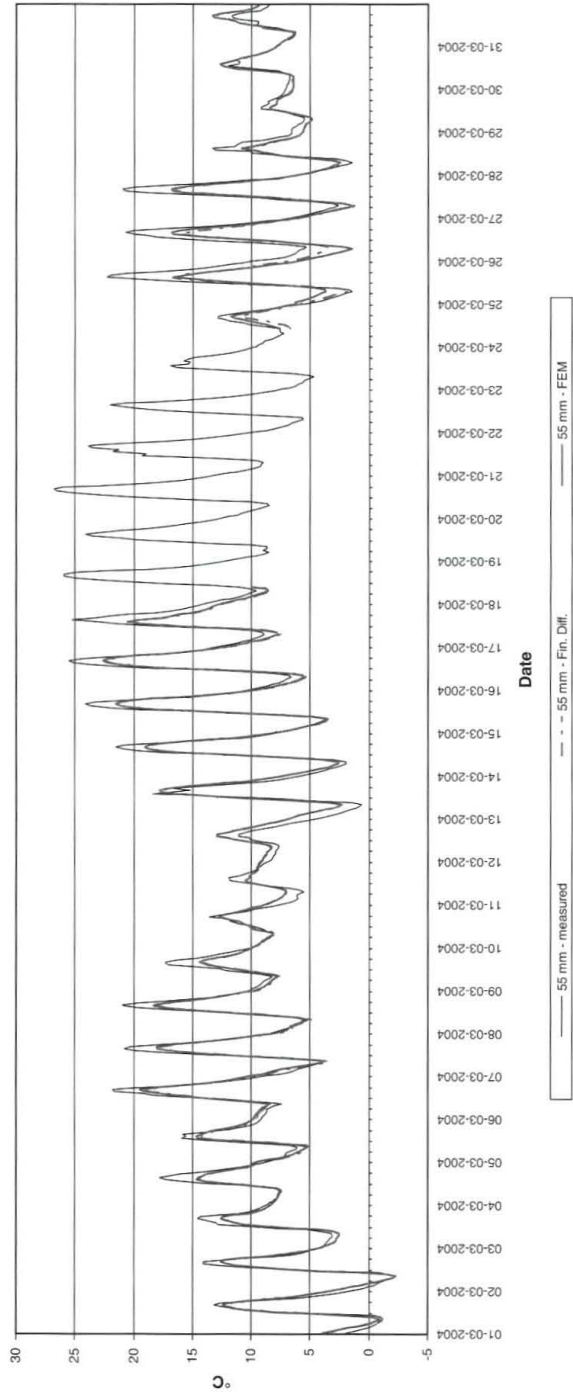


FIGURE 8 March 55-mm depth temperature distribution (Fin. Diff. = finite differences method).

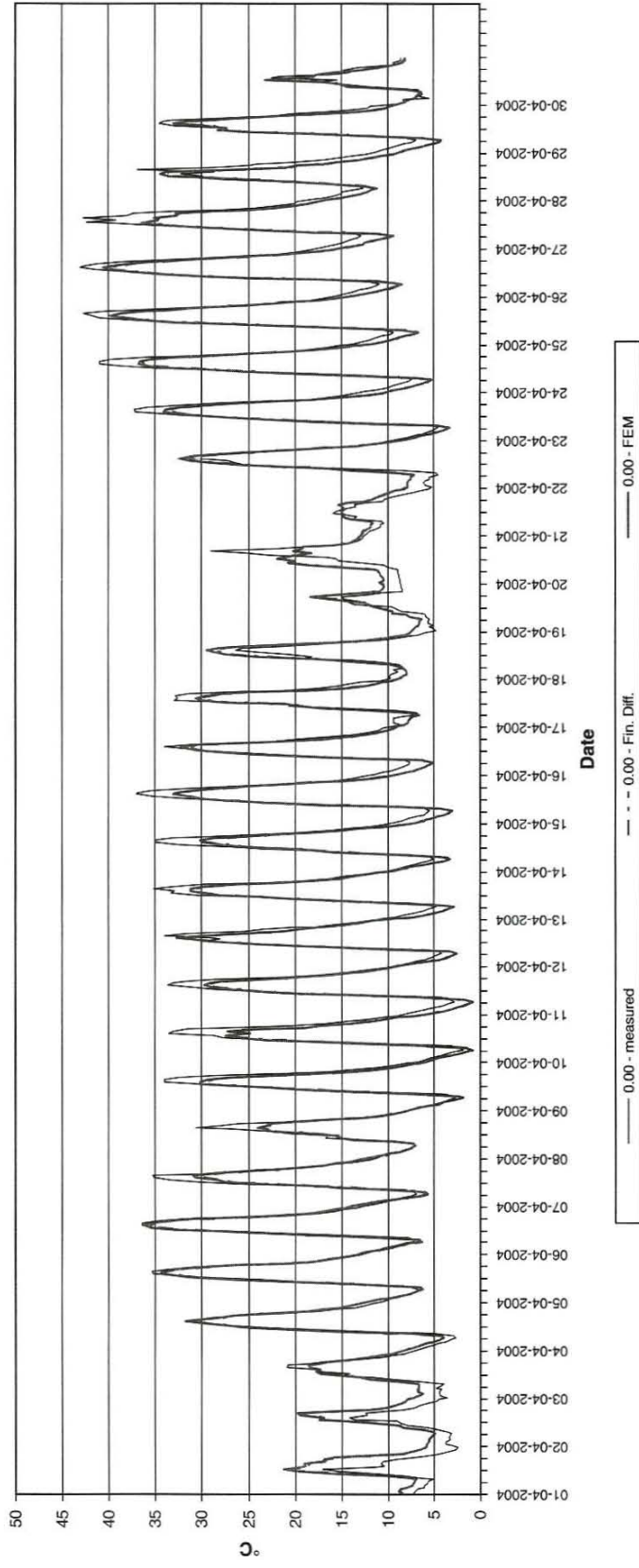


FIGURE 9 April 0.0-mm depth temperature distribution (Fin. Diff. = finite differences method).

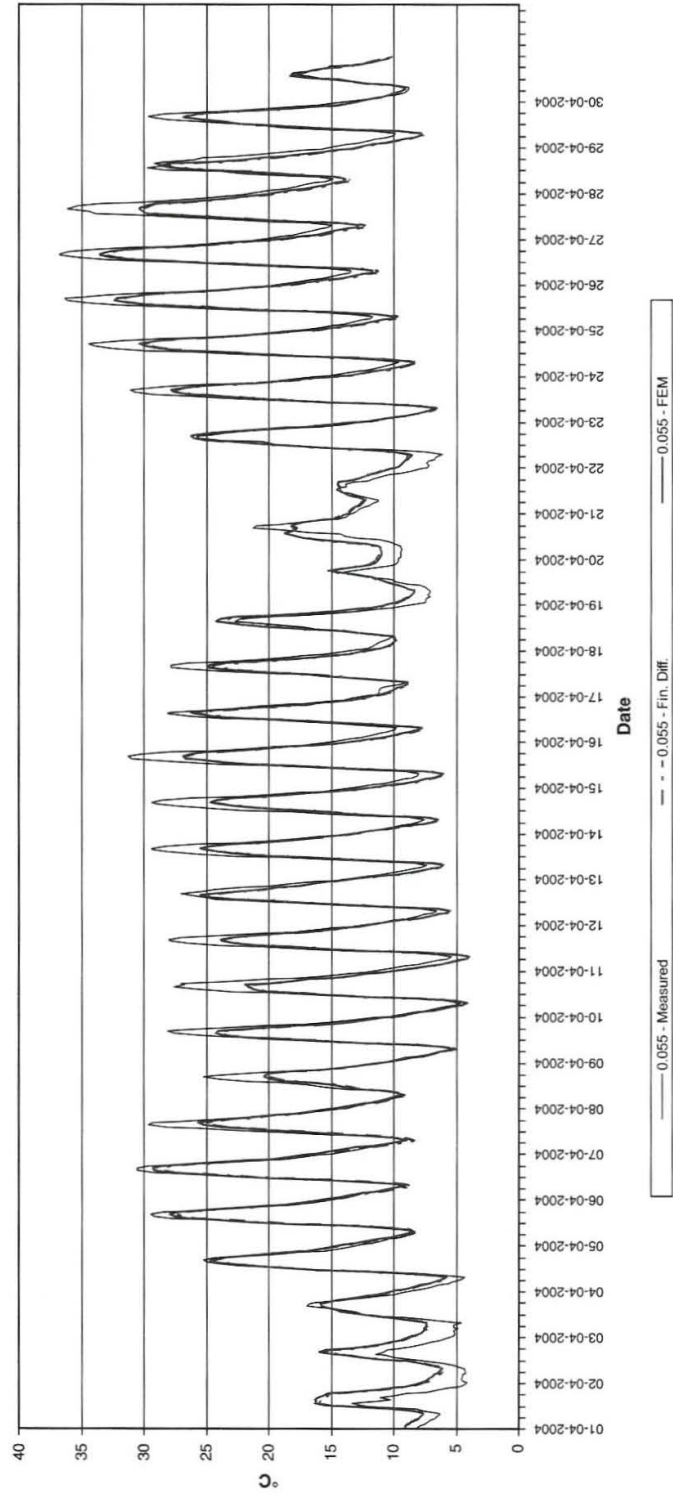


FIGURE 10 April 55-mm depth temperature distribution (Fin. Diff. = finite differences method).

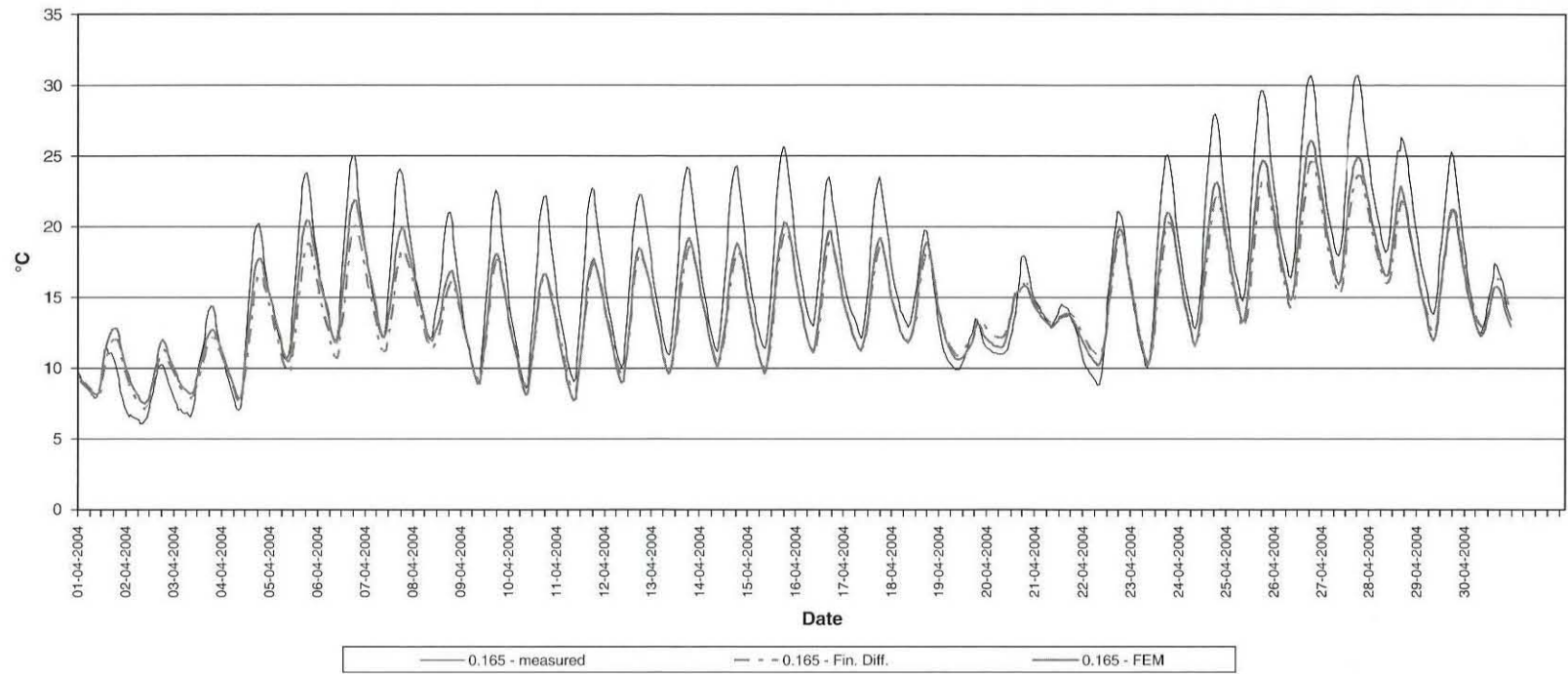


FIGURE 11 April 165-mm depth temperature distribution (Fin. Diff. = finite differences method).

3D FEM model also produces good results when compared with models of one-dimensional nature.

#### ACKNOWLEDGMENT

The authors acknowledge the work and technical support from the Bragança delegation of the Portuguese Road Administration.

#### REFERENCES

1. Sousa, J. B., J. C. Pais, R. Saim, G. B. Way, and R. N. Stubstad. Mechanistic-Empirical Overlay Design Method for Reflective Cracking. In *Transportation Research Record: Journal of the Transportation Research Board, No. 1809*, Transportation Research Board of the National Academies, Washington, D.C., 2002, pp. 209–217.
2. de Bondt, A. Effect of Reinforcement Properties. *Proc., PRO11 4th International RILEM Conference on Reflective Cracking in Pavements—Research in Practice* (A. O. Abd Halim, D. A. Taylor, and H. H. Mohamed, ed.), RILEM, Ottawa, Ontario, Canada, 2000, pp. 13–22.
3. Shalaby, A., A. O. Abd El Halim, and S. M. Easa. Low-Temperature Stresses and Fracture Analysis of Asphalt Overlays. In *Transportation Research Record 1539*, TRB, National Research Council, Washington, D.C., 1996, pp. 132–139.
4. Mrawira, D. M., and J. Luca. Thermal Properties and Transient Temperature Response of Full-Depth Asphalt Pavements. In *Transportation Research Record: Journal of the Transportation Research Board No. 1809*, Transportation Research Board of the National Academies, Washington, D.C., 2002, pp. 160–169.
5. Dewitt, D. P., and F. P. Incropera. *Fundamentals of Heat and Mass Transfer*, 4th ed. John Wiley and Sons, New York, 1996.
6. Özisik, M. N. *Heat Transfer: A Basic Approach*. McGraw-Hill, New York, 1985.
7. Hermansson A. Mathematical Model for Calculation of Pavement Temperatures: Comparisons of Calculated and Measured Temperatures. In *Transportation Research Record: Journal of the Transportation Research Board, No. 1764*, TRB, National Research Council, Washington, D.C., 2001, pp. 180–188.
8. Picado-Santos, L. *Consideração da Temperatura no Dimensionamento de Pavimentos Rodoviários Flexíveis* [in Portuguese]. Ph.D. thesis. University of Coimbra, Lisbon, Portugal, 1994.
9. Minhoto, M. J. C., J. C. Pais, P. A. A. Pereira, and L. G. Picado-Santos. Low-Temperature Influence in the Predicted Pavement Overlay Life. Presented at Asphalt Rubber 2003 Conference, Brasilia, Brasil, 2003, pp. 167–180.
10. ANSYS 5.6 [computer program]. ANSYS Theory Reference—Release 5.6. Edited by Peter Kohnke. ANSYS, Inc., Canonsburg, Pa., 1999.

*The Flexible Pavement Design Committee sponsored publication of this paper.*

**TRANSPORTATION RESEARCH RECORD:  
JOURNAL OF THE TRANSPORTATION RESEARCH BOARD**

**Peer Review Process**

The *Transportation Research Record: Journal of the Transportation Research Board* publishes approximately 30% of the more than 2,500 papers that are peer reviewed each year. The mission of the Transportation Research Board (TRB) is to disseminate research results to the transportation community. The Record series contains applied and theoretical research results as well as papers on research implementation.

The TRB peer review process for the publication of papers allows a minimum of 30 days for initial review and 60 days for rereview, to ensure that only the highest-quality papers are published. At least three reviews must support a committee's recommendation for publication. The process also allows for scholarly discussion of any paper scheduled for publication, along with an author-prepared closure.

The basic elements of the rigorous peer review of papers submitted to TRB for publication are described below.

**Paper Submittal: June 1–August 1**

Papers may be submitted to TRB at any time. However, most authors use the TRB web-based electronic submission process available between June 1 and August 1, for publication in the following year's Record series.

**Initial Review: August 15–October 31**

TRB staff assigns each paper by technical content to a committee that administers the peer review. The committee chair assigns at least three knowledgeable reviewers to each paper. The initial review is completed by mid-September.

By October 1, committee chairs make a preliminary recommendation, placing each paper in one of the following categories:

1. Publish as submitted or with minor revisions,
2. Publish pending author changes and rereview, or
3. Reject for publication.

By late October, TRB communicates the results of the initial review to the corresponding author indicated on the paper submission form. Corresponding authors communicate the information to coauthors. Authors of papers in Category 2 (above) must submit a revised version addressing all reviewer comments and must include a cover letter explaining how the concerns have been addressed.

**Rereview: November 20–January 25**

The committee chair reviews revised papers in Category 1 (above) to ensure that the changes are made and sends the Category 2 revised papers to the initial reviewers for rereview. After rereview, the chairs make the final recommendation on papers in Categories 1 and 2. If the paper has been revised to the committee's satisfaction, the chair will recommend publication. The chair communicates the results of the rereview to the authors.

**Discussion: February 1–May 1**

After the Annual Meeting, discussions may be submitted for papers that will be published. TRB policy is to publish the paper, the discussion, and the author's closure in the same Record.

Attendees interested in submitting a discussion of any paper presented at the TRB Annual Meeting must notify TRB no later than February 1. If the paper has been recommended for publication, the discussion must be submitted to TRB no later than March 1. A copy of this communication is sent to the author and the committee chair.

The committee chair reviews the discussion for appropriateness and asks the author to prepare a closure to be submitted to TRB by April 1. The committee chair reviews the closure for appropriateness. After the committee chair approves both discussion and closure, the paper, the discussion, and the closure are included for publication together in the same Record.

**Final Manuscript Submittal: April 1**

In early February, TRB requests a final manuscript for publication—to be submitted by April 1—or informs the author that the paper has not been accepted for publication. All accepted papers are published by December 31.

**Paper Awards: April to January**

The TRB Executive Committee has authorized annual awards sponsored by Groups in the Technical Activities Division for outstanding published papers:

- Charley V. Wootan Award (Policy and Organization Group);
- Pyke Johnson Award (Planning and Environment Group);
- K. B. Woods Award (Design and Construction Group);
- Patricia F. Waller Award (Safety and System Users Group);
- D. Grant Mickle Award (Operations and Maintenance Group);

and

- John C. Vance Award (Legal Resources Group).

Other Groups also may nominate published papers for any of the awards above. In addition, each Group may present a Fred Burggraf Award to authors 35 years of age or younger.

Peer reviewers are asked to identify papers worthy of award consideration. Each Group reviews all papers nominated for awards and makes a recommendation to TRB by September 1. TRB notifies winners of the awards, which are presented at the following TRB Annual Meeting.

**TRB Annual Meeting**

The majority of papers are submitted to TRB for both publication and presentation. Chairs of committees that review papers for publication also make recommendations on presentations. After completion of the initial review, in addition to making the preliminary publication recommendations, chairs make presentation recommendations. This ensures high-quality paper sessions at the Annual Meeting. Authors of all papers on the program are asked to submit the revised versions of their papers electronically for a CD-ROM distributed at the Annual Meeting.

**Transportation Research Board  
www.TRB.org**

**TRANSPORTATION RESEARCH BOARD**

500 Fifth Street, NW  
Washington, DC 20001

---

ADDRESS SERVICE REQUESTED

**THE NATIONAL ACADEMIES™**

*Advisers to the Nation on Science, Engineering, and Medicine*

The nation turns to the National Academies—National Academy of Sciences, National Academy of Engineering, Institute of Medicine, and National Research Council—for independent, objective advice on issues that affect people's lives worldwide.

[www.national-academies.org](http://www.national-academies.org)